Available online at www.sciencedirect.com
ScienceDirect
Biochemical and Biophysical Research Communications 352 (2007) 213–219
BBRC
www.elsevier.com/locate/ybbrc

ATR microspectroscopy with multivariate analysis segregates grades of exfoliative cervical cytology

Michael J. Walsh [a], Maneesh N. Singh [a,b], Hubert M. Pollock [c], Leanne J. Cooper [a], Matthew J. German [d], Helen F. Stringfellow [b], Nigel J. Fullwood [a], Evangelos Paraskevaidis [e], Pierre L. Martin-Hirsch [b], Francis L. Martin [a,*]

[a] *Biomedical Sciences Unit, Lancaster University, Lancaster, UK*
[b] *Lancashire Teaching Hospitals, NHS Trust, Preston, UK*
[c] *Department of Physics, Lancaster University, Lancaster, UK*
[d] *School of Dental Sciences, Newcastle University, Newcastle upon Tyne, UK*
[e] *Department of Obstetrics and Gynecology, University of Ioannina, Ioannina, Greece*

Received 1 November 2006
Available online 9 November 2006

Abstract

Although cervical cancer screening in the UK has led to reductions in the incidence of invasive disease, this programme remains flawed. We set out to examine the potential of infrared (IR) microspectroscopy to allow the profiling of cellular biochemical constituents associated with disease progression. Attenuated total reflection-Fourier Transform IR (ATR) microspectroscopy was employed to interrogate spectral differences between samples of exfoliative cervical cytology collected into liquid based cytology (LBC). These were histologically characterised as normal ($n = 5$), low-grade ($n = 5$), high-grade ($n = 5$) or severe dyskaryosis (? carcinoma) ($n = 5$). Examination of resultant spectra was coupled with principal component analysis (PCA) and subsequent linear discriminant analysis (LDA). The interrogation of LBC samples using ATR microspectroscopy with PCA–LDA facilitated the discrimination of different categories of exfoliative cytology and allowed the identification of potential biomarkers of abnormality; these occurred prominently in the IR spectral region 1200 cm^{-1}–950 cm^{-1} consisting of carbohydrates, phosphate, and glycogen. Shifts in the centroids of amide I ($\approx$1650 cm^{-1}) and II ($\approx$1530 cm^{-1}) absorbance bands, indicating conformational changes to the secondary structure of intracellular proteins and associated with increasing disease progression, were also noted. This work demonstrates the potential of ATR microspectroscopy coupled with multivariate analysis to be an objective alternative to routine cytology.

Keywords: ATR microspectroscopy; Cervical cancer; Cervical intra-epithelial neoplasia; Exfoliative cytology; Principal component analysis; Screening

The introduction of cervical cancer screening in the UK has led to significant reductions in both incidence and mortality from this disease [1]. It meets many prerequisites required for a screening programme in that it facilitates the detection of treatable pre-malignant stages before invasion occurs [2]. However, due to inadequacies in specificity and sensitivity, current screening practices remain flawed. Best screening tests are those which have a high level of sensitivity (i.e., positive when there is disease) and best confirmatory diagnostic tests are those that have high levels of specificity (i.e., negative when disease is not present) [3].

Pre-malignant pathology in the cervix is designated in the UK as cervical intra-epithelial neoplasia (CIN) and with increasing severity, graded as CIN1, CIN2 or CIN3. In other regions (e.g., USA) CIN1 is also known as a low-grade squamous intraepithelial lesion (LSIL); such lesions may regress and often do not require treatment. Likewise, CIN2 and CIN3 may be known as high-grade squamous intraepithelial lesion (HSIL); this categorisation

* Corresponding author. Fax: +44 1524 593192.
E-mail address: f.martin@lancaster.ac.uk (F.L. Martin).

0006-291X/$ - see front matter © 2006 Elsevier Inc. All rights reserved.
doi:10.1016/j.bbrc.2006.11.005

of pathology requires treatment upon diagnosis [4]. Liquid based cytology (LBC) in cervical cancer screening is now used in the UK. This differs from the conventional technique that involves smearing exfoliated cells directly onto a glass slide [5]. Exfoliated cells may now be transferred into a fixative known as ThinPrep (Cytyc Corporation) or SurePath (TriPath Care Technologies); LBC is used to reduce occurrence of inadequate smears [6]. Misdiagnosis can occur due to lack of training, poor management or tiredness [7].

Infrared (IR) microspectroscopy appears to be applicable in cervical cancer diagnostics [8–10]; this allows the acquisition of a "biochemical-cell fingerprint" [11]. Biomolecules absorb in the mid-IR (2–20 μm), giving vibrational spectra that contain absorbance intensity peaks corresponding to different chemical bonds [8–22]. Thus IR microspectroscopy can allow the detection of DNA, RNA, lipids, phosphate and carbohydrate levels [11]. This fingerprint appears to increasingly alter as a cell progresses through pre-malignant stages from normal to invasive disease [8]. The identification of an absorbance intensity peak or ratio of peaks may allow the identification of a biomarker for pre-malignancy or cancer [12]. Attenuated total reflection-Fourier Transform IR (ATR) microspectroscopy allows the fast acquisition of spectra with a high signal-to-noise ratio (SNR) and allows the interrogation of individual groups of cells, high-density samples and complex cell membranes [12]. Photothermal microspectroscopy (PTMS) is another mid-IR method, currently in development, that appears capable of achieving sub-cellular resolution [11,23,24].

We employed ATR microspectroscopy to determine whether we could segregate spectra derived from different categories of exfoliative cytology. LBC samples were obtained from 20 donors and 10 spectra were derived per sample (200 spectra in total). The samples fell into four categories: normal ($n = 5$ donors), low-grade (CIN1, $n = 5$), high-grade (CIN2/3, $n = 5$), and severe dyskaryosis (? carcinoma, $n = 5$). Our aim was to determine whether a spectral fingerprint of exfoliative cytology in LBC ThinPrep fixative could be employed to identify differences associated with pre-malignant stages of cervical cancer and, whether these could be discriminated using multivariate data analysis.

Methods

Study samples. Samples of exfoliative cytology were collected into the ThinPrep fixative (Preserv Cyt™ solution, Cytyc Corp., Boxborough, MA, USA). Informed consent to obtain samples for research was obtained (LREC No. 05/Q1308/2; Preston, Chorley and South Ribble Ethical Committee).

LBC clean-up for ATR microspectroscopy. Exfoliated cytology samples in ThinPrep fixative were centrifuged at 1500 rpm for 5 min. ThinPrep fixative, which was found to possess an IR spectral signature in the 900 cm^{-1}–1800 cm^{-1} region of interest (see Supplemental data), was aspirated carefully leaving behind the residual cell pellet. Three wash steps were subsequently conducted; these each consisted of (1) the addition of 3 ml of autoclaved H_2O, (2) re-suspension of cellular material, (3) centrifugation at 1500 rpm for 5 min and (4) aspiration of supernatant. This clean-up procedure was found to eliminate the ThinPrep spectral signature from the sample. The resultant pellet was re-suspended in 0.5 ml of autoclaved H_2O and this cellular suspension was then applied to 1 cm × 1 cm Low-E glass microscope slides (Kevley Technologies, Chesterland, OH, USA). Allowed to dry in a sterile environment overnight, the microscope slides with adhered cellular material were then transferred to a dessicator until analysis with ATR microspectroscopy.

ATR microspectroscopy. ATR IR spectra were acquired using the Bruker Vector 22 FTIR spectrometer with Helios ATR attachment containing a diamond crystal (Bruker Optics Ltd, Coventry, UK). Using a CCTV camera attached to the ATR crystal, 10 random points were interrogated. Data were collected in ATR mode and spectra (8 cm^{-1} spectral resolution, co-added for 32 scans) were converted into absorbance using Bruker OPUS software. Sodium dodecyl sulphate was used to clean the ATR crystal prior to the first spectral analysis of each sample. Each spectrum had background absorption automatically subtracted, were baseline corrected and were normalised to the amide I (≈1650 cm^{-1}) absorbance peak using OPUS software. Average spectra were also derived using OPUS software.

Statistical analysis. Raw spectra were processed employing principal component analysis (PCA) performed using the Pirouette software package (Infometrix Inc., Woodinville, USA). Grouping of spectra into clusters and the extent to which these clusters correspond to classes of sample is derived. PCA is built on the assumption that variation implies information: it replaces the original several hundred wavenumbers with just a very few significant new variables or principal components (PCs). PCs are automatically listed in order, according to how much of the original data variance is accounted for by each one. For each spectrum obtained, each of the many readings (one for each wavenumber) is replaced by a "score," one for each PC. Thus in a scores plot, each set of measurements (spectrum) appears as a single point in n-dimensional space, whose coordinates are its scores on the one, two or more significant PCs chosen as axes for the plot. PCAs allow one to identify the wavenumbers that contribute to inter-spectral variation: plots showing the extent to which each wavenumber contributes to a given PC provide the necessary pseudo-spectrum or loadings plot.

As suggested by Fearn [25], we used PCA for preliminary data reduction and processed the output using linear discriminant analysis (LDA). In LDA, new variables are found such that the ratio of the between-cluster variance to the within-cluster variance is maximised, so that the clusters appear at maximum separation. LDA has the additional advantage in that it allows the choice of predetermined classes (i.e., category of cytology or identity of patient) to be taken into account during the derivation of clusters and loading plots.

We analysed for differences between the different categories of cytology (class variable determined by category) and for differences within different categories (i.e., between different patients in the same category: class variable determined by patient). Scores plots were derived for the spectral region 1850 cm^{-1}–900 cm^{-1}.

Results and discussion

Differences between normal, low-grade, high-grade, and severe dyskaryosis (? carcinoma) exfoliative cytology were observed in IR spectra (≈1850 cm^{-1}–900 cm^{-1}) (Fig. 1A). Comparison of these ATR spectra derived from different LBC categories suggested that differences were concentrated between ≈1200 cm^{-1} and 950 cm^{-1}. These were associated with a glycogen peak (≈1030 cm^{-1}), a carbohydrate peak (≈1155 cm^{-1}), a phosphate peak (≈1080 cm^{-1}) and degree of protein phosphorylation (≈970 cm^{-1}). There also appeared to be a progressive shift in the centroid of the amide I peak (≈1650 cm^{-1}) of low-grade, high-grade, and dyskaryosis (? carcinoma) spectra (Fig. 1B and C). Such

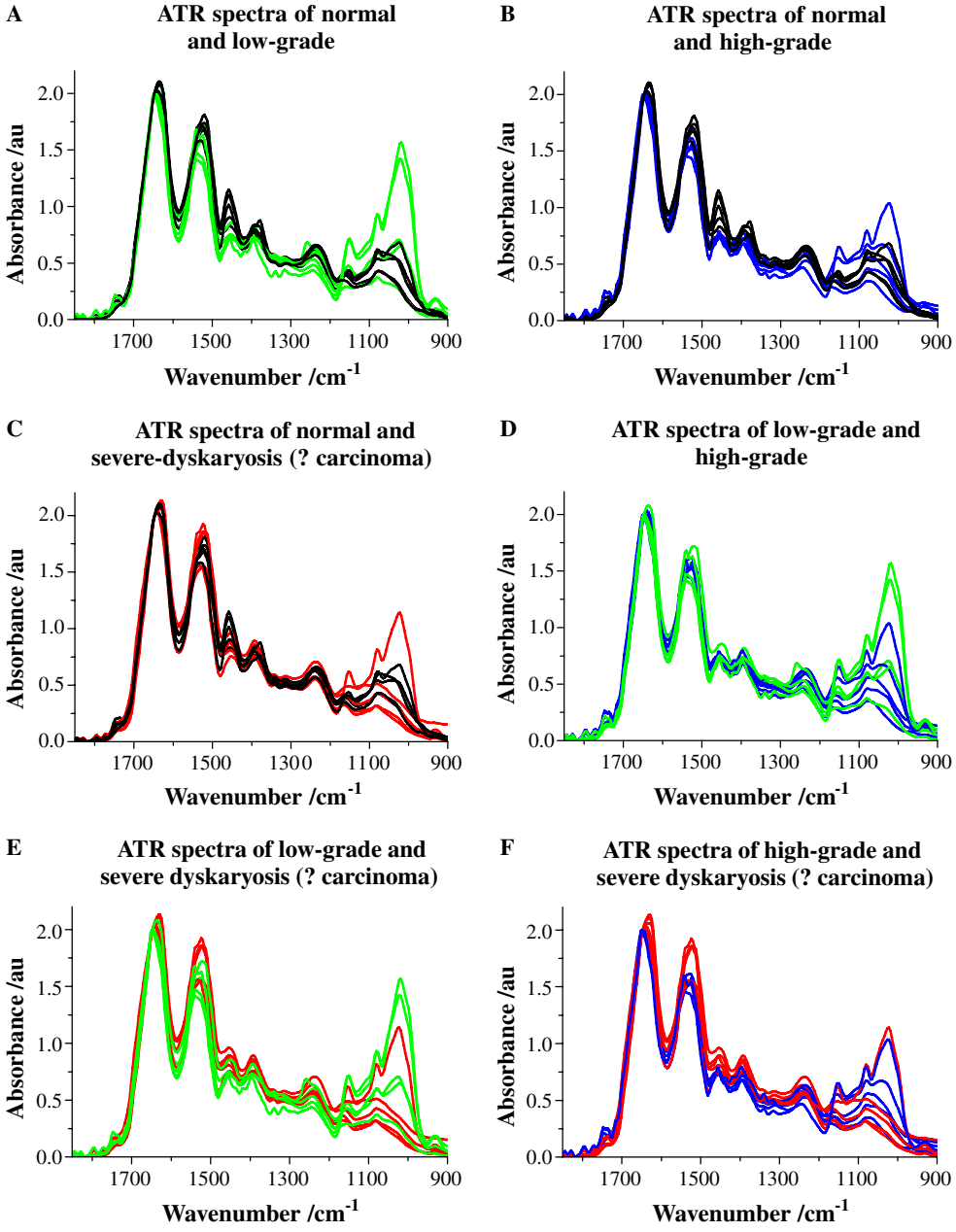

Fig. 1. Average absorbance spectra of the biochemical-cell fingerprint region (1850 cm^{-1}–900 cm^{-1}) comparing all four categories of exfoliative cytology: (A) normal (black) and low-grade (green); (B) normal and high-grade (blue); (C) normal and severe dyskaryosis (? carcinoma, red); (D) low-grade and high-grade; (E) low-grade and severe dyskaryosis (? carcinoma); and (F) high-grade and severe dyskaryosis (? carcinoma).

a shift in the amide I absorbance band (≈5 cm^{-1}) may be due to changes in the secondary structure of intracellular proteins. The amide II absorbance band also appeared to exhibit a large degree of variation, with a reduced intensity associated with low-grade and high-grade compared to normal (Fig. 1B and C) and a striking reduction in the comparison of high grade and severe dyskaryosis (? carcinoma) (Fig. 1F).

Fig. 2 shows scores plots calculated from data classed by was patient. The different patient clusters show excellent separation. Even within a given category, there is marked inter-patient variation: this is not surprising, given that the variables that distinguish the various patients include not only the category of cytology, but other confounding factors. Spectra from different categories of cytology separated significantly and this is particularly clear when normal and low-grade exfoliative cytology was examined (Fig. 2A). Good separation was also observed when comparing normal patient clusters to high-grade or dyskaryosis (? carcinoma) patient clusters (Fig. 2B and C). When low-grade samples were compared with high-grade, separation of the low-grade patient clusters was observed despite the

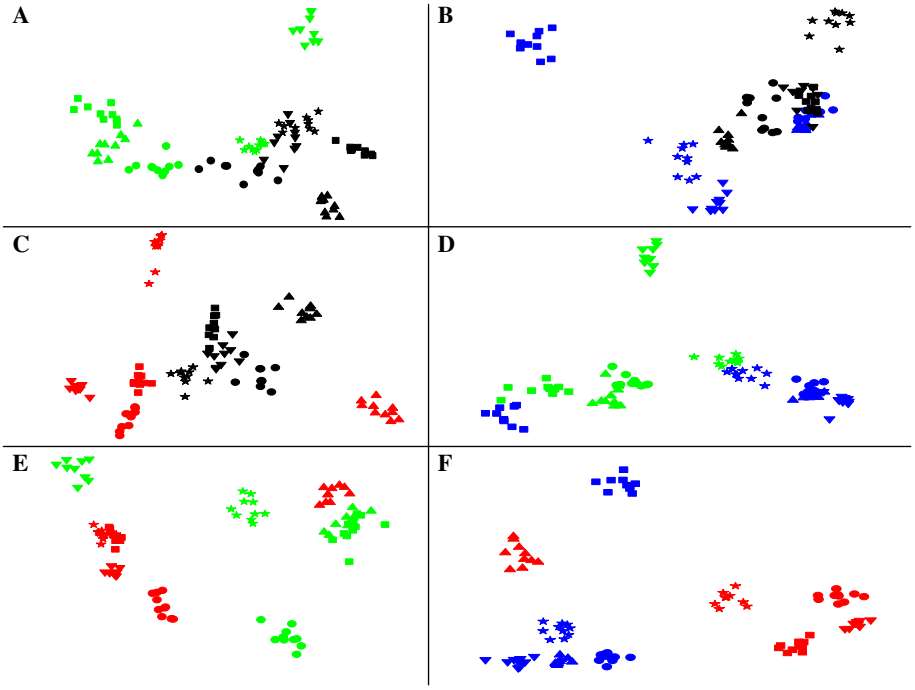

Fig. 2. PCA–LDA scores plots, classed by patient (each symbol represents data from one patient, and each point corresponds to one spectrum): (A) normal (black) and low-grade (green); (B) normal and high-grade (blue); (C) normal and severe dyskaryosis (? carcinoma, red); (D) low-grade and high-grade; (E) low-grade and severe dyskaryosis (? carcinoma); (F) high-grade and severe dyskaryosis (? carcinoma).

fact that high-grade spectra exhibited a degree of heterogeneity as shown by some separation between different patient spectral groups within this category (Fig. 2D). There was again separation between low-grade and severe dyskaryosis (? carcinoma) patient clusters (Fig. 2E). Spectra from high-grade samples were also observed to cluster separately from severe dyskaryosis (? carcinoma) samples (Fig. 2F).

PCA–LDA yielded loadings plots that identify the principal wavenumbers responsible for spectral separation. The data were classed by category of cytology, without distinction between patients within a given category. The most informative loadings plots were those that resulted from analysis of two categories at a time, where each curve shows the principal wavenumbers at which mean spectra from all samples in each of the categories of exfoliative cytology differ (Fig. 3A–F). Fig. 4A shows the PCA–LDA scores plot, as in Fig. 2, but in this instance, all the derived spectra ($n = 200$) from the cohort of donor samples ($n = 20$) analysed were classed by category of cytology and were viewed according to maximum clustering. Some degree of cluster separation is seen, but probably as a consequence of inter-individual differences this does not result in complete segregation. In addition, Fig. 4B shows the loadings plots derived from analyses where the spectra from each LBC category were compared with the mean of all spectra.

Possible biomarkers of progression were identified. In general, the greatest degree of variance was accounted for by absorbance bands associated with the degree of protein phosphorylation at 970 cm^{-1}, glycogen at 1030 cm^{-1}, and shifts in the centroid of amide I $\approx$ 1650 cm^{-1}, indicating their important contribution to cluster separation. Categories including normal showed evidence of significance variance in the 1400 cm^{-1}–1650 cm^{-1} region; however, with low-grade, high-grade and severe dyskaryosis (? carcinoma) cytology additional significant peaks were observed between 950 cm^{-1} and 1300 cm^{-1} (Fig. 4B). When normal was compared to low-grade, wavenumbers at 970 cm^{-1}, 1030 cm^{-1} and 1080 cm^{-1} were particularly significant causes of variance (Fig. 3A); compared to high grade, variance was noted at 970 cm^{-1}, 1030 cm^{-1} and 1530 cm^{-1} (Fig. 3B); and compared to severe dyskaryosis (? carcinoma), significant variance was noted throughout the 900 cm^{-1}–1850 cm^{-1} spectral region (Fig. 3C). Again, when low-grade was compared to high-grade cytology the most significant variance was concentrated in the 950 cm^{-1}–1200 cm^{-1} spectral region (Fig. 3D) whereas when low-grade versus severe dyskaryosis (? carcinoma) was examined, significant variance was noted throughout the 900 cm^{-1}–1850 cm^{-1} spectral region (Fig. 3E). Of note is the fact that variance between normal and low-grade is much greater than that observed between low-grade and high-grade; this might suggest that the former transition is the more important step towards transformation. When high-grade cytology was compared to severe dyskaryosis (? carcinoma), significant variance was observed mostly in the 950 cm^{-1}–1200 cm^{-1} spectral region (Fig. 3F).

Likely biomarkers of severe dyskaryosis (? carcinoma) were also identified. A significant peak at 1030 cm^{-1}, due

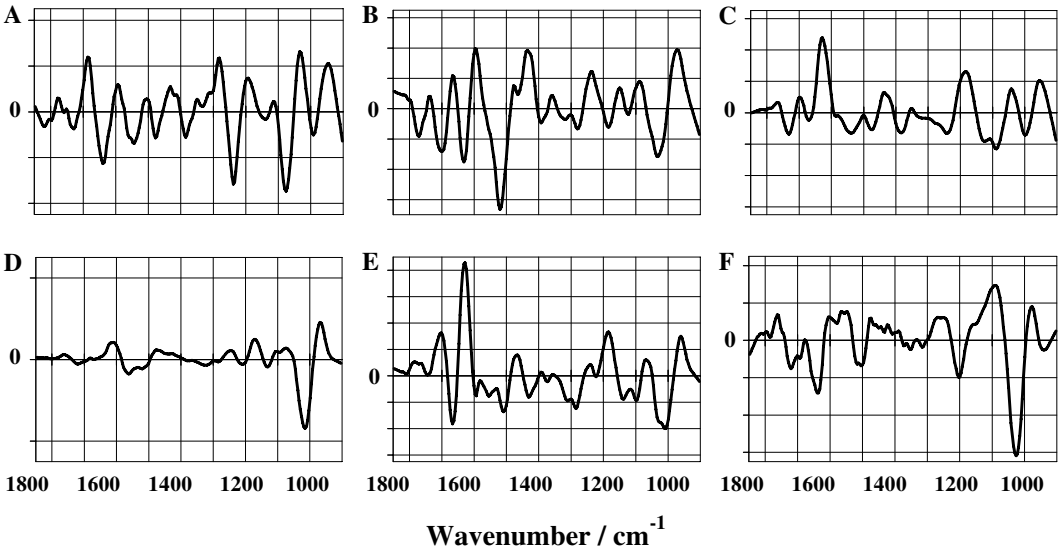

Fig. 3. Loadings plots of spectra averaged and classed by category, analysed by PCA–LDA two categories at a time. Each curve shows the principal wavenumbers at which mean spectra from all samples in each of two categories of exfoliative cytology differ: (A) normal versus low-grade; (B) normal versus high-grade; (C) normal versus severe dyskaryosis (? carcinoma); (D) low-grade versus high-grade; (E) low-grade versus severe dyskaryosis (? carcinoma); (F) high-grade versus severe dyskaryosis (? carcinoma). The same *y*-scale (in arbitrary units) is used for each plot, as a measure of how much variation each wavenumber contributes to the relevant cluster vector.

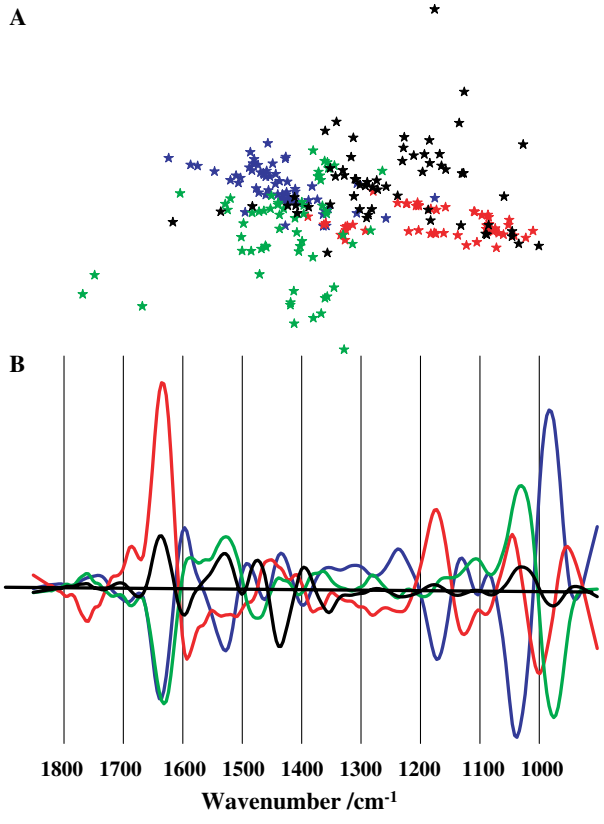

Fig. 4. Data from samples in all four categories of exfoliative cytology, averaged and classed by category before analysis by PCA–LDA: (A) PCA–LDA scores plot, as in Fig. 2 but classed by category (black, normal; green, low-grade; blue, high-grade; red, severe dyskaryosis (? carcinoma)); (B) loadings plots, where spectra from each category are compared with the mean of all spectra (black, normal; green, low-grade; blue, high-grade; red, severe dyskaryosis (? carcinoma)).

to glycogen, was observed when comparing high-grade cytology to severe dyskaryosis (? carcinoma) (Fig. 3F). Amide I and amide II were also shown to be important contributors to variance in severe dyskaryosis (? carcinoma) comparisons, with peaks observed between 1650 cm^{-1} and 1550 cm^{-1} (Fig. 3C, E, and F). Loadings plots comparing severe dyskaryosis (? carcinoma) against all categories showed variance throughout the spectral region (Fig. 4B).

With PCA alone, spectral separation was achieved and was associated with peaks corresponding to amide I (≈1650 cm^{-1}), amide II (≈1540 cm^{-1}), carbohydrates (≈1155 cm^{-1}), symmetric phosphate (≈1080 cm^{-1}) and glycogen (≈1030 cm^{-1}) (data not shown). Symmetric phosphate and glycogen were the dominating factors in spectral segregation. Of note was the fact that protein phosphorylation (≈970 cm^{-1}) was not observed to contribute to variance although, using PCA–LDA this became a major contributing factor. PCA–LDA gives clearer clustering and separation compared to PCA alone and does this employing a specific algorithm. With a PCA scores plot, the user is required to make a selection of PCs and to rotate the plot in order to identify the best view; this is not a fully objective procedure. PCA–LDA allows the spectral features responsible for cluster separation between designated classes to be objectively found. This may identify factors underlying inter-category differences and those that might point to variance between samples within a category.

Cervical smears consist of squamous and columnar epithelial cells; however, other interfering factors are often present, e.g., erthryocytes, leukocytes, bacteria, yeast, and mucin [26]. The presence of these may alter the composi-

tion of derived IR spectra [27]. However, using ATR microspectroscopy we obtained excellent segregation of different categories of exfoliative cervical cytology with minimal sample preparation. ATR microspectroscopy is adaptable for high-throughput analysis with minimal sample preparation. The ATR crystal covers a ≈250 μm × 250 μm surface area and thus, acquired spectra provide a representative analysis of the whole smear [28]. The possibility to perform *in vivo* tissue analysis also exists [29–31]. Our findings using ATR microspectroscopy coupled with PCA–LDA suggests a novel, objective alternative to current visual screening techniques for diagnosis of exfoliative cytology.

Acknowledgments

This work was funded by Rosemere Cancer Foundation (M.J.W., M.S., and P.L.M.-H.) and EPSRC Grant GR/S75918/01 (H.M.P., M.J.G., and F.L.M.). We thank Dr. A. Hammiche (Lancaster University) for expert technical help and, Dr. J.M. Chalmers (VS Consulting) and Prof. T. Fearn (University College London) for essential advice on PCA and LDA, respectively.

Appendix A. Supplementary data

Supplementary data associated with this article can be found, in the online version, at doi:10.1016/j.bbrc.2006.11.005.

References

[1] M. Quinn, P. Babb, J. Jones, E. Allen, Effect of screening on incidence of and mortality from cancer of cervix in England: evaluation based on routinely collected statistics, B.M.J. 318 (1999) 04–908.
[2] J. Peto, C. Gilham, O. Fletcher, F.E. Matthews, The cervical cancer epidemic that screening has prevented in the UK, Lancet 364 (2004) 249–256.
[3] K. Nanda, D.C. McCrory, E.R. Myers, L.A. Bastian, V. Hasselblad, J.D. Hickey, D.B. Matchar, Accuracy of the Papanicolaou test in screening for and follow-up of cervical cytologic abnormalities: asystematic review, Ann. Intern. Med. 132 (2000) 810–819.
[4] A.G. Oster, Natural history of cervical intraepithelial neoplasia: a critical review, Int. J. Gynecol. Pathol. 12 (1993) 86–192.
[5] J. Karnon, J. Peters, J. Platt, J. Chilcott, E. McGoogan, N. Brewer, Liquid-based cytology in cervical screening: an updated rapid and systematic review and economic analysis, Health Technol. Assess. 8 (2004) 1–78.
[6] E. Davey, A. Barratt, L. Irwig, S.F. Chan, P. Macaskill, P. Mannes, A.M. Saville, Effect of study design and quality on unsatisfactory rates, cytology classifications, and accuracy in liquid-based versus conventional cervical cytology: a systematic review, Lancet 367 (2006) 122–132, doi:10.1016/S0140-6736(06)67961-0, [Online 12, January 2006].
[7] G.G. Birdsong, Automated screening of cervical cytology specimens, Hum. Pathol. 27 (1996) 468–481.
[8] M.J. Walsh, M.J. German, M. Singh, H.M. Pollock, A. Hammiche, M. Kyrgiou, H.F. Stringfellow, E. Paraskevaidis, P.L. Martin-Hirsch, F.L. Martin, IR microspectroscopy: potential applications in cervical cancer screening, Cancer Lett. 246 (2007) 1–11; doi:10.1016/j.canlet.2006.03.019, [Online 19, May 2006].
[9] M.J. Tobin, M.A. Chesters, J.M. Chalmers, F.J. Rutten, S.E. Fisher, I.M. Symonds, A. Hitchcock, R. Allibone, S. Dias-Gunasekara, Infrared microscopy of epithelial cancer cells in whole tissues and in tissue culture, using synchrotron radiation, Faraday Discuss 126 (2004) 27–39.
[10] R.K. Sahu, S. Argov, A. Salman, U. Zelig, M. Huleihel, N. Grossman, J. Gopas, J. Kapelushnik, S. Mordechai, Can Fourier transform infrared spectroscopy at higher wavenumbers (mid IR) shed light on biomarkers for carcinogenesis in tissues? J. Biomed. Opt. 10 (2005) 54017–54026.
[11] A. Hammiche, M.J. German, R. Hewitt, H.M. Pollock, F.L. Martin, Monitoring cell cycle distributions in MCF-7 cells using near-field photothermal microspectroscopy, Biophys. J. 88 (2005) 699–3706, doi:10.1529/biophysj.104.053926, [Online 18, February 2005].
[12] M.J. German, A. Hammiche, N. Ragavan, M.J. Tobin, L.J. Cooper, S.S. Matanhelia, A.C. Hindley, C.M. Nicholson, N.J. Fullwood, H.M. Pollock, F.L. Martin, IR spectroscopy with multivariate analysis potentially facilitates the segregation of different types of prostate cells, Biophys. J. 90 (2006) 3783–3795, doi:10.1529/biophysj.105.077255, [Online 24, February 2006].
[13] P.T.T. Wong, R.K. Wong, T.A. Caputo, T.A. Godwin, B. Rigas, Infrared-spectroscopy of exfoliated human cervical cells—evidence of extensive structural-changes during carcinogenesis, Proc. Natl. Acad. Sci. USA 88 (1991) 10988–10992.
[14] M.A. Cohenford, B. Rigas, Cytologically normal cells from neoplastic cervical samples display extensive structural abnormalities on IR spectroscopy: implications for tumor biology, Proc. Natl. Acad. Sci. USA 95 (1998) 15327–15332.
[15] S. Argov, J. Ramesh, A. Salman, I. Sinelikov, J. Goldstein, H. Guterman, S. Mordechai, Diagnostic potential of Fourier-transform infrared microspectroscopy and advanced computational methods in colon cancer patients, J. Biomed. Opt. 7 (2002) 248–254.
[16] M.J. Romeo, B.R. Wood, M.A. Quinn, D. McNaughton, Removal of blood components from cervical smears: implications for cancer diagnosis using FTIR spectroscopy, Biopolymers 72 (2003) 69–76.
[17] S. Mordechai, R.K. Sahu, Z. Hammody, S. Mark, K. Kantarovich, H. Guterman, A. Podshyvalov, J. Goldstein, S. Argov, Possible common biomarkers from FTIR microspectroscopy of cervical cancer and melanoma, J. Microsc. 215 (2004) 86–91.
[18] E. Gazi, J. Dwyer, N. Lockyer, P. Gardner, J.C. Vickerman, J. Miyan, C.A. Hart, M. Brown, J.H. Shanks, N. Clarke, The combined application of FTIR microspectroscopy and ToF-SIMS imaging in the study of prostate cancer, Faraday Discuss. 126 (2004) 41–59.
[19] A. Tfayli, O. Piot, A. Durlach, P. Bernard, M. Manfait, Discriminating nevus and melanoma on paraffin-embedded skin biopsies using FTIR micro spectroscopy, Biochim. Biophys. Acta 1724 (2005) 62–269.
[20] D.C. Fernandez, R. Bhargava, S.M. Hewitt, I.W. Levin, Infrared spectroscopic imaging for histopathologic recognition, Nat. Biotech. 23 (2005) 469–474.
[21] A. Podshyvalov, R.K. Sahu, S. Mark, K. Kantarovich, H. Guterman, J. Goldstein, R. Jagannathan, S. Argov, S. Mordechai, Distinction of cervical cancer biopsies by use of infrared microspectroscopy and probabilistic neural networks, Appl. Opt. 44 (2005) 3725–3734.
[22] M. Diem, S. Boydston-White, L. Chiriboga, Infrared spectroscopy of cells and tissues: shining light onto a novel subject, Appl. Spectrosc. 53 (1999) 148A–161A.
[23] A. Hammiche, L. Bozec, M.J. German, J.M. Chalmers, N.J. Everall, G. Poulter, M. Reading, D.B. Grandy, F.L. Martin, H.M. Pollock, Mid-infrared microspectroscopy of difficult samples using near-field photothermal microspectroscopy, Spectroscopy 19 (2004) 20–42.
[24] H.M. Pollock, D.A. Smith, The use of near-field probes for vibrational spectroscopy and photothermal imaging, in: J.M. Chalmers, P.R. Griffiths (Eds.), Handbook of Vibrational Spectroscopy, vol. 2, Wiley, New York, 2002, pp. 1472–1492.
[25] T. Fearn, Discriminant analysis, in: J.M. Chalmers, P.R. Griffiths (Eds.), Handbook of Vibrational Spectroscopy, vol. 3, Wiley, NewYork, 2002, pp. 2086–2093.
[26] B. Young, J.W. Heath, Wheaters Functional Histology, fourth ed., Churchill Livingstone.

[27] M.J. Romeo, M.A. Quinn, F.R. Burden, D. McNaughton, Influence of benign cellular changes in diagnosis of cervical cancer using IR microspectroscopy, Biopolymers 67 (2002) 362–366.
[28] S.R. Lowry, The analysis of exfoliated cervical cells by infrared microscopy, Cell. Mol. Biol. 44 (1998) 169–177.
[29] J.R. Mourant, R.R. Gibson, T.M. Johnson, S. Carpenter, K.W. Short, Y.R. Yamada, J.P. Freyer, Methods for measuring the infrared spectra of biological cells, Phys. Med. Biol. 48 (2003) 243–257.
[30] M. Miljkovic, M. Romeo, C. Matthaus, M. Diem, Infrared microspectroscopy of individual human cervical cancer (HeLa) cells suspended in growth medium, Biopolymers 74 (2004) 172–175.
[31] D.A. Moss, M. Keese, R. Pepperkok, IR microspectroscopy of live cells, Vib. Spectrosc. 38 (2005) 185–191.